Modern Applied Science; Vol. 9, No. 4; 2015
ISSN 1913-1844 E-ISSN 1913-1852
Published by Canadian Center of Science and Education

Numerical Cavitation Model for Simulation of Mass Flow Stabilization Effect in ANSYS CFX

Sergey Yurievich Konstantinov[1], Dmitry Vladimirovich Tselischev[1] & Vladimir Aleksandrovich Tselischev[1]

[1] Ufa State Aviation Technical University, Russia

Correspondence: Dmitry Vladimirovich Tselischev, Ufa State Aviation Technical University, Russia. E-mail: nuked@mail.ru

Received: October 30, 2014 Accepted: November 6, 2014 Online Published: December 10, 2014

doi:10.5539/mas.v9n4p21 URL: http://dx.doi.org/10.5539/mas.v9n4p21

Abstract

The aim of the article is improvement of numerical cavitation models for simulation of an effect of cavitation stabilization of fluid mass flow. The methods of development of a new dynamic component for a numerical model of cavitation mass transfer is presented in the paper. Application of the new method resulted in a new dynamic component for numerical model of cavitation mass transfer, which takes into account fluid viscosity in Reley-Plesset equation. Relying on the methods being considered fundamentally new hydroautomatic devices such as cavitation mass flow stabilizers and flow dividers could be designed. The new dynamic component has become the basis for the new numerical model of cavitation mass transfer. The effect of cavitation stabilization of fluid mass flow was simulated by this dynamic component. The numerical model was verified by experimental researches of the effect of cavitation stabilization of fluid mass flow in a jet element "pipe-pipe". The results of simulation showed that the new numerical model of cavitation mass transfer can simulate the jet pipes with the difference between results of simulation and experiment not exceeding 2,5% and visualizing a cavitation zone more adequate.

Keywords: cavitation, cavitation mass transfer, numerical model of cavitation, mass flow stabilization, Reley-Plesset equation

1. Introduction

1.1 Effect of Cavitation Stabilization of Fluid Mass Flow

Hydraulic and fuel systems development requires fundamentally new hydroautomatic devices, using the multiphase flows effects in work process. One of these effects is gas-dynamic crisis of an outflow of the vapor-fluid flow (Nigmatullin, 1988, Wallis, 1969), also called the cavitation stabilization of fluid mass flow (Tselischev V. et al., 1998).

Cavitation stabilization of fluid mass flow is a positive effect of hydrodynamic cavitation, resulting in "flow choking" at inlet constant pressure and at outlet variable pressure. This effect is not observed at inlet variable pressure and at outlet constant pressure.

Stabilization of mass flow can be widely applied in hydrodrives for constant speed of hydraulic actuator regardless of load and flow division. However relation of stabilization mass flow with the inlet pressure and geometry limits the use of the effect and requires designing a cavitation element for a certain hydraulic system.

During the cavitation element design there arises a problem of defining stabilization mass flow and stabilization zone width for the given geometry. Currently the stabilization mass flow and stabilization zone width can be defined by experiments and numerical simulation.

1.2 Hypotheses Explaining the Effect of Cavitation Stabilization of Fluid Mass Flow

There are three hypotheses explaining the mass flow stabilization effect 1) "crisis" of two-phase vapor-liquid flow; 2) return stream; 3) boundary layer retention.

Hypothesis of crisis" of two-phase vapor-liquid flow was first proposed by Wallis (Wallis G. B., 1969). It is based on analogy between critical outflow from conic nozzle and cavitation stabilization effect of mass flow. By this hypothesis the gas and fluid mixture becomes critical during the cavitation, if the mass flow can't be changed by modifying channel outlet pressure at fixed parameters of flow braking. According to the hypothesis the critical mixture has flow velocity equal to sound speed. Calculation of mass flow stabilization by the hypothesis of "crisis" of a two-phase flow is precise up to the pressure of 10 - 15 atm., at a higher pressure the error grows. The problem of the hypothesis is the need for experimental estimation of phases volume fractions and vapor and liquid velocities. This explains error increase at higher pressures.The hypothesis of return streams (Tselischev, 2006) supposes that there can emerge a zone with developed cavitation phenomena provided that the working fluid has sufficient amount of cavitation bubbles around walls of a reception nozzle of a jet element. The zone is characterized by local change of pressure due to bubbles collapse. When pressure rises intensive return streams are observed in the reception nozzle. Moving on the periphery of the main flow the return streams try to leave the diffuser channel, but they have to pass the cavitation zone. If the counter-pressure in the diffuser nozzle is not sufficient, the return stream cannot pass this zone and has to resist the pressure together with the main stream of liquid, i.e. the cavitation prevents return streams from flowing away and enables to stabilize the mass flow.

The hypothesis of preservation of boundary layer supposes that the jet pipe forms an axisymmetric turbulent stream with almost rectangular profile of velocity at the jet camera inlet. If the pressure in the jet camera is equal to pressure in the reception nozzle (a zero pressure gradient between the reception nozzle and the jet camera) the theory of free submerged turbulent streams can be used to describe the flow. The turbulent stream forms a jet boundary layer in the jet camera which is accruing in the interval between the two nozzles. When the stream reaches the reception nozzle, two scenarios are possible: 1) with cavitation switched off a jet boundary layer with thickness about 0,35 - 0,5 of the reception nozzle radius becomes unstable and breaks up; 2) with cavitation switched on the liquid density in the boundary layer falls and it is retained till escaping from the nozzle due to the concentration of cavitation bubbles at reception nozzle walls. Due to cavitation in the main stream the boundary layer is retained on the walls of the cavitating element resulting in the effect of mass flow stabilization.

A jet-cavitation fluid mass flow stabilizer (Bocharov et al., 1987) is the most promising device. It involves the effect of cavitation stabilization of fluid mass flow in its work process and is an analog of a mass flow valve (flow-control valve). The main obstacle for the use of the stabilizer is absence of analytical calculations of hydraulic characteristics.

The purpose of the paper is improvement of numerical cavitation models for simulation of the cavitation effect of mass flow stabilization.

1.3 Methods of Numerical Simulation of Cavitation

During the cavitation simulation two concepts should be distinguished: cavitation model and model of cavitation mass transfer (Sauer, 2000). Cavitation model is a complex of equations, describing the cavitation flow and mass transfer in it. Model of cavitation mass transfer is the model of mass transfer mechanism during phase transfer, or vaporization during the cavitation. There are two methods of numerical simulation of cavitation: Method of moving boundary (Interface tracking) and Method of continuum (Interface capturing) (Wursthorn, 2001).

During the simulation by Interface tracking method between vapor and fluid phases the boundary is formed, which moves depending on mass transfer. Flow simulation is performed only for liquid phase, vapor phase is considered to be fixed.

During simulation by Interface capturing method between vapor and fluid phases interfacial area is formed, in which volume fractions of vapor and fluid are variable. Model of mass transfer allows to evaluate volume fractions of vapor and fluid in the interfacial area and determine its size.

1.4 Mathematical Model of the Cavitation Mass Transfer

A moderrn numerical model of the cavitation mass transfer based on a Reley equation, evaluates volume fraction of vapor and fluid in a cell. The model takes into account two factors: a bubble dynamic and statistic character of a bubbles distribution in cavitation flow.

A dynamic of bubble growth (collapse) is evaluated by simplified Reley equation (Brennen, 1995):

$$\frac{dR}{dt} = \sqrt{\frac{2}{3}\frac{p_B - p}{\rho_l}} = \sqrt{\frac{2}{3}\frac{\Delta p}{\rho_l}}\ , \tag{1}$$

where R – cavitation bubble radius; p_B – pressure inside bubble (saturated vapor pressure in the model); p – pressure in fluid (absolute pressure in a solver); ρ – fluid density; Δp – pressure drop affecting the bubble.

To eliminate instability the cavitation simulation with low Courant number (25 – 50) is used. But this method increases time of simulation and is of help only in 30 – 40% of cases (Permyakov and Tselischev D., 2010). A similar method is a physical timescale assignment during the cavitation simulation in ANSYS CFX. As a result, the CFD-packages developers could not guarantee a convergence of the simulation for specific terms and geometry.

Statistical character of the cavitation flow is taken into account through a vapor volume fraction in the cell, quantity of bubble nuclei and their initial radius (Schnerr et al., 1999):

$$\alpha = n \cdot \frac{4}{3} \pi R_0^{\ 3}, \tag{2}$$

where n – quantity of the bubbles in the cell; R_0 – initial radius of cavitation bubble; α – vapor volume fraction in the cell.

As the quantity of cavitation bubbles in the volume at a certain time of simulation is unknown the problem could be solved by introducing some initial radius of the bubble R_0 that will modify a type of the static component of model:

$$n = \frac{3\alpha}{4R_0^{\ 3}\pi}, \tag{3}$$

Singhal et al. (2001) proposed the use of the statistical component in the following way:

$$F\frac{\max(1,\sqrt{k})(\alpha)}{\sigma} \cdot \rho_l \rho_{vap}, \tag{4}$$

where F – vaporization (condensation) coefficient; σ – surface tension coefficient; k – pressure relaxation coefficient; ρ_l – fluid density; ρ_{vap} – vapor density.

Because of coefficient k the model had a poor convergence which resulted in a number of works on modification of the statistical component.

Zwart, Gerber, Belamri (2004) proposed the following form of the statistical component:

$$F_{vap}\frac{3\alpha_{nuc}(1-\alpha_{vap})\rho_{vap}}{R_0} \tag{5}$$

where α_{nuc}= $5 \cdot 10^{-4}$ – coefficient of a link of the vapor volume fraction with vapor mass fraction.

Schnerr (2001) has modified the statistical component in view of fluid and vapor density, which allows simulating the cavitation in fluids comparable with their vapors by density:

$$\frac{\rho_{vap}\rho_l}{\rho}\alpha(1-\alpha)\frac{3}{R_0}. \tag{6}$$

It should be noted that during the entire time of existence of numerical cavitation models there were no attempts to modify a dynamic component, due to the absence of a common solution of Reley and Reley-Plesset equations.

2. Materials and Methods

Creation of a new numerical model of cavitation mass transfer has four stages:

1) Initial data setting; 2) Simulation of non-dimensional speed depending on Reynolds number;3) Approximation of non-dimensional speed of a bubble growth by three approximating functions; 4) Synthesis of a new dynamic component of the numerical model of cavitation mass transfer.

On the first stage initial data are set, such as:

1) Pressure drops interval, for which the numerical model of cavitation mass transfer is corrected. The interval is assigned by lower and upper values;

2) Step of pressure drop;

3) Physical properties of the fluid (viscosity μ, density ρ), for which the dynamic component of the numerical model of cavitation mass transfer are corrected;

4) Non-dimensional time of the end of cavitation bubble growth takes the value from 2 till 10 (Levkovsky, 1978).

The second stage makes it possible to calculate the dependence of non-dimensional speed of the cavitation bubble growth on Reynolds number. The stage consists of three parts:

1) Solution of non-dimensional Reley-Plesset equation for the bubble growth in view of fluid viscosity:

$$b\frac{d^2b}{d\tau^2}+\frac{3}{2}\left(\frac{db}{d\tau}\right)^2+\frac{1}{Re\cdot b}\frac{db}{d\tau}=1\,, \tag{7}$$

where b – non-dimensional radius of the cavitation bubble; Re – Reynolds number for the cavitation bubble; τ – non-dimensional time of the cavitation bubble growth.

Reynolds number, non-dimensional radius and non-dimensional time of growth are expressed as (Levkovsky, 1978):

$$Re=\frac{R_0\sqrt{\Delta p\cdot\rho}}{4\mu};\quad b=\frac{R}{R_0};\quad \tau=\frac{t}{R_0}\sqrt{\frac{\Delta p}{\rho}}, \tag{8}$$

where $R_0 = 10^{-6}$m – initial radius of the bubble; R – current radius of the bubble.

2) The results of the solution (1) are combined into the common variable – a two-dimensional array.

3) The results of the calculation are displayed in the form of a diagram.

On the stage of approximation the dependences of non-dimensional growth speed are approximated by three functions.

Approximation function #1:

$$\frac{db}{d\tau}=f(Re)=\sqrt{\frac{2}{3}}\,\mathrm{tgh}(w_2\cdot Re^{w_1})\,, \tag{9}$$

where w_1 and w_2 – approximation coefficients.

Approximation function #2:

$$\frac{db}{d\tau}=f(Re)=\sqrt{\frac{2}{3}}\,\mathrm{tgh}(w_1\cdot Re)\,, \tag{10}$$

where w_1 – approximation coefficient.

Approximation function #3:

$$\frac{db}{d\tau}=f(Re)=\sqrt{\frac{2}{3}}(\mathrm{tgh}(w_1\cdot Re^{w_2})+w_3\cdot Re^{w_4})\,, \tag{11}$$

where w_1, w_2, w_3, w_4 – approximation coefficients.

The approximation is done by means of mathematical software, for example Maple (Waterloo Maple Inc.).

Approximation results in approximation coefficients and an approximation error. Each approximation function is compared in the diagram with non-dimensional speed of the cavitation bubble growth depending on Reynolds number, which was calculated on the stage #2.

On the fourth stage a new dynamic component for numerical model of cavitation mass transfer is synthesized by the formula:

$$\frac{dR}{dt}=\frac{db}{d\tau}\sqrt{\frac{\Delta p}{\rho}}\,. \tag{12}$$

The result of the method is dependence of growth speed of cavitation bubble on viscosity and density of the fluid. The dependence is calculated in view of pressure drop Δp and initial radius of the bubble R_0.

Synthesis of the new dynamic component for numerical model of cavitation mass transfer is carried out in pressure interval from 100 till 10^6 Pa with pressure step 1000 Pa for water density 1000 kg/m^3 and viscosity 1 cSt. The new dynamic component will be used in numerical model of cavitation mass transfer in CFD-package ANSYS CFX.

After calculation, the approximation function #1 becomes:

$$\frac{db}{d\tau}=f(Re)=\sqrt{\frac{2}{3}}\cdot\mathrm{tgh}(1,221\cdot Re^{0,353})\,, \tag{13}$$

approximation function #2 becomes:

$$\frac{db}{d\tau} = f(Re) = \sqrt{\frac{2}{3}} \cdot \mathrm{tgh}(1,428 \cdot Re), \tag{14}$$

approximation function #3 becomes:

$$\frac{db}{d\tau} = f(Re) = \sqrt{\frac{2}{3}} \cdot (\mathrm{tgh}(1,734 \cdot Re^{0,457}) - 0,078 \cdot Re^{-0,610}). \tag{15}$$

Accordingly approximation error for function #1 is 6,36%, for function #2 is 42,08%, for function #3 is 0,08%. Function #3 has the closest approximation but when entering the program code of the CFD-package ANSYS CFX it becomes too complicated. So function #1 should be taken as its approximation error is 6,36%.

The dynamic component for numerical model of cavitation mass transfer in view of the chosen approximation function #1 changes to:

$$\frac{dR}{dt} = \sqrt{\frac{2}{3}} \cdot \mathrm{tgh}(1,221 \cdot \left(\frac{R_0\sqrt{\Delta p \cdot \rho}}{4\mu}\right)^{0,353}) \cdot \sqrt{\frac{\Delta p}{\rho}}. \tag{16}$$

Thus, this method results in a new dynamic component for numerical model of cavitation mass transfer taking into account fluid viscosity.

In view of (16) and the statistical component of the Zwart-Gerbert-Belamri model (5) the new model of cavitation mass transfer becomes:

$$\begin{aligned} p < p_н, m_e &= F_{vap} \frac{3\alpha_{nuc}(1-\alpha_{vap})\rho_{vap}}{R_0} \cdot \mathrm{tgh}(1.22(\frac{R_0\sqrt{(p_н - p)\rho}}{4\mu})^{0.35}) \cdot \sqrt{\frac{2}{3}\frac{p_н - p}{\rho_l}}; \\ p > p_н, m_c &= F_{cond} \frac{3\alpha_{vap}\rho_{vap}}{R_0} \cdot \mathrm{tgh}(1.22(\frac{R_0\sqrt{(p_н - p)\rho}}{4\mu})^{0.35}) \cdot \sqrt{\frac{2}{3}\frac{p - p_н}{\rho_l}}. \end{aligned} \tag{17}$$

3. Results

3.1 Numerical Simulation of Cavitating Flow

Object of numerical simulation and experimental research is the jet element of "pipe-pipe" type with parameters: $d = 1.6$ mm; $\bar{d} = 1.25$; $\bar{h} = 0.93$.

For numerical simulation the cavitation model based on Interface capturing method was used (Zwart et al., 2004). The model consists of mass balance equation, momentum equation and turbulence model. Mass balance equation has the form:

$$\begin{aligned} \frac{\partial \alpha\rho_\alpha}{\partial t} + div(\alpha\rho_\alpha\vec{v}) &= -m_{e(c)} \\ \frac{\partial \beta\rho_\beta}{\partial t} + div(\beta\rho_\beta\vec{v}) &= m_{e(c)} \end{aligned}, \tag{18}$$

where α – fluid volume fraction; β – vapor volume fraction; ρ_α – fluid density; ρ_β – vapor density; $m_{e(c)}$ – mass source obtained by calculation of mass transfer equation.

To pass from mass balance equation (18) to continuity equation for subcavitating flow the following correlation is introduced:

$$\alpha + \beta = 1 \tag{19}$$

Taking into account mass balance equation (19) the momentum equation becomes:

$$\begin{aligned} \frac{\partial(\alpha\rho_\alpha\vec{v})}{\partial t} + div(\alpha\rho_\alpha\vec{v} \otimes \vec{v}) &= -\alpha\nabla p_\alpha + \alpha\nabla\tau_\alpha - m_{e(c)}\vec{v}, \\ \frac{\partial(\beta\rho_\beta\vec{v})}{\partial t} + div(\beta\rho_\beta\vec{v} \otimes \vec{v}) &= -\beta\nabla p_\beta + \beta\nabla\tau_\beta + m_{e(c)}\vec{v} \end{aligned} \tag{20}$$

Pressure in a point is calculated by generalized Stocks hypothesis:

$$p = -\frac{1}{3}(p_{xx} + p_{yy} + p_{zz}). \tag{21}$$

Shear stress tensor in fluid is calculated by the following way:

$$\tau = \mu \cdot (\nabla \vec{v} + (\nabla \vec{v})^T - \frac{2}{3} div(\vec{v})) . \quad (22)$$

Viscosity is calculated by the following equation:

$$\mu = \mu_0 + \mu_t . \quad (23)$$

Turbulent viscosity value is calculated by turbulence model. For simulation of cavitation in local hydraulic resistances $k - \varepsilon$ model based on Boussinesq hypothesis is the most relevant.

Turbulent viscosity in $k - \varepsilon$ model is calculated through turbulent kinetic energy k and rate of its dissipation ε:

$$\mu_t = \frac{C_\mu \rho k^2}{\varepsilon} , \quad (24)$$

Turbulent kinetic energy and dissipation rate are calculated by the following equations:

$$\begin{aligned} &\frac{\partial}{\partial t}(\alpha \rho_\alpha k_\alpha) + \nabla \cdot (\alpha(\rho_\alpha \vec{v} k_\alpha - (\mu + \frac{\mu_{t\alpha}}{\sigma_k}) \nabla k_\alpha)) = \alpha(P_\alpha - \rho_\alpha \varepsilon_\alpha) + T_\alpha^{\ k} , \\ &\frac{\partial}{\partial t}(\alpha \rho_\alpha \varepsilon_\alpha) + \nabla \cdot (\alpha(\rho_\alpha \vec{v} \varepsilon_\alpha - (\mu + \frac{\mu_{t\alpha}}{\sigma_k}) \nabla \varepsilon_\alpha)) = \alpha \frac{\varepsilon_\alpha}{k_\alpha}(C_{\varepsilon 1} P_\alpha - C_{\varepsilon 2} \rho_\alpha \varepsilon_\alpha) + T_\alpha^{\ \varepsilon} , \end{aligned} \quad (25)$$

where $C_{\varepsilon 1} = 1.44$, $C_{\varepsilon 2} = 1.92$, $\sigma_k = 1$, $\sigma_\varepsilon = 1.22$.

Numerical simulation was performed in CFD-package ANSYS CFX with pressure in jet camera 9 bar and outlet pressure 101 bar. Pressure in outlet varied from 10 to 95 bar with the step of 10 bar. Working fluid temperature was 32°C. Working fluid parameters: hydraulic oil Shell T46 with density 872 kg/m^3 and viscosity 80 sSt. Simulation mesh contained 2 801 1363 of nodes. Residual values (errors) with which the simulation was considered to be converged were 10^{-5}.

Simulation was performed in three series of 10 simulations: 1) by cavitation model switched off; 2) by Zwart-Gerber-Belamri (ZGB) cavitation model switched on:

$$\begin{aligned} &p < p_н , m_e = F_{vap} \frac{3 \alpha_{nuc} (1 - \alpha) \rho_{vap}}{R_0} \cdot \sqrt{\frac{2}{3} \frac{p_н - p}{\rho_l}} , \\ &p > p_н , m_c = F_{cond} \frac{3 \alpha \rho_{vap}}{R_0} \cdot \sqrt{\frac{2}{3} \frac{p - p_н}{\rho_l}} ; \end{aligned} \quad (26)$$

3) by new model of cavitation mass transfer (17), by «interface capturing» using the turbulence model k-[epsilon].

3.2 Method of Experimental Research

Experimental researches were carried out on the base of Training Science and Information Center “Gidropnevmoavtomatika” at VPO “USATU” on the test bench “Diagnosis and identification of hydraulic systems”, made by “Hydac” (Poland).

The jet element “pipe-pipe” was installed and fixed on the test bench. Connection was provided by scheme presented on Figure 1.

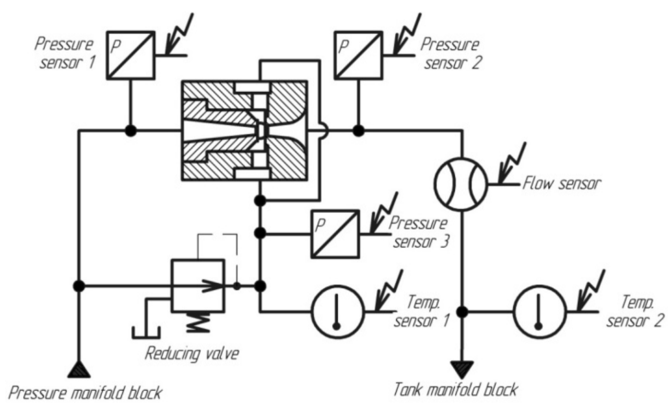

Figure 1. Scheme of connection of jet element (stabilizer) to test bench

The stabilizer input was connected to Pressure manifold block; output was connected to Tank manifold block that had a throttle to set the outlet pressure. Jet camera was connected to a reducing valve providing constant pressure during the experiment. Experimental results were recorded automatically by a universal measuring system HYDAC HMG 3000 with test frequency 50 hertz. Flow, pressure and temperature data as well as time step were saved to a file.

At the beginning of experiment when the throttle of the Tank manifold block was closed the pressure level at the stabilizer input was 100 bar. When the throttle opened the pressure in jet camera became 8 bar. Since the moment when inlet pressure became 100 bar and pressure in jet camera became 8 bar the throttle started to close and data recording began. The data recording stopped when the throttle fully closed. Experimental results were processed in package DIAdem (National Instruments) with filtration, smoothing and approximation.

3.2 Results of Experimental Research

P-Q characteristic curve of simulation of various cavitation models, when cavitation model was switched on and in comparison with experimental data are shown in Figure 2. The curve has an evident effect of cavitation stabilization of mass flow (characteristic fracture). *P-Q* characteristic curve when cavitation model was switched off defines the boundary of cavitation starting at pressure change from 60 to 70 bar. *P-Q* characteristic curve with cavitation model switched on diverged insignificantly with the experiment (1 – 1,2%), which is due to features of the design. The fracture of the curve without cavitation can be explained by the fact that the jet being closed by pressure in the receiving nozzle resulted in fluid mass flow increase while passing through the jet camera.

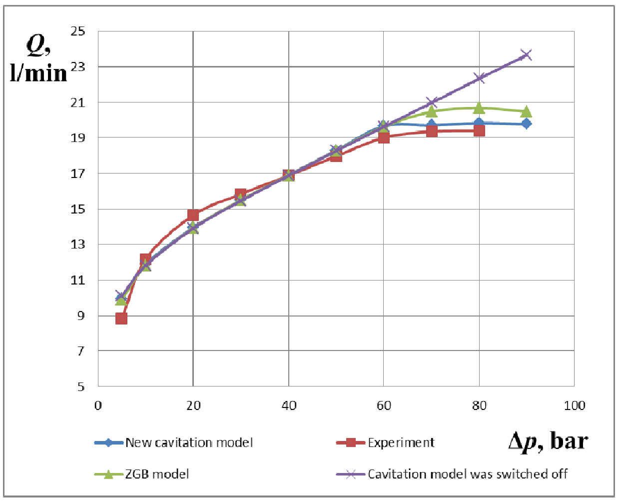

Figure 2. Numerical simulation of cavitation stabilization of mass flow compared with experiment

Fields of velocities visualization, obtained during numerical simulation with cavitation model switched on and switched off are presented in Figure 3.

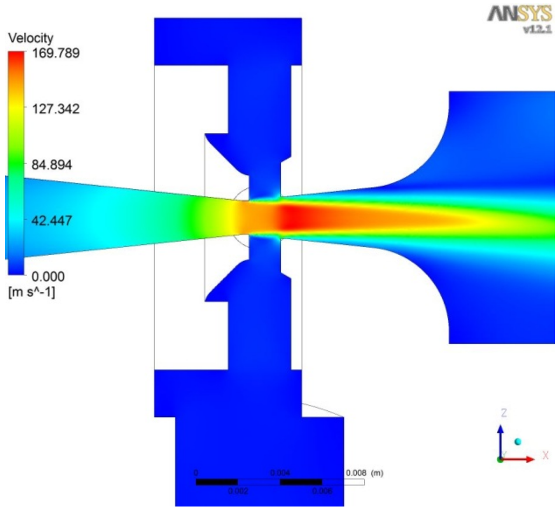

a) cavitation model was switched off

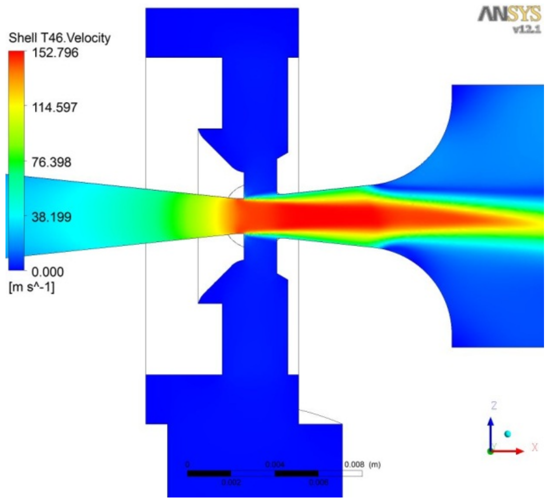

b) cavitation model was switched on (a new cavitation model)

Figure 3. Fields of velocities visualization, obtained during numerical simulation of fluid flow through jet element “pipe-pipe” with pressure drop 90 bar with cavitation model switched off and by a new cavitation model

Analysis of figure 3 shows a qualitative change of boundary layer along the receiving nozzle during flow simulations with cavitation switched on and off. During the flow simulation with cavitation switched off the boundary layer formed in the jet camera enters the receiving nozzle for 1-2 mm and disintegrates because of great thickness.

During flow simulation with cavitation model switched on the boundary layer is filled by vapor and is retained up to detachment from receiving nozzle. Fluid mass flow through the jet outlet is determined by fluid mass flow that enters the receiving nozzle. Thus in the case the boundary layer is retained the fluid mass flow becomes constant which enables to explain the mass flow stabilization effect by preservation of the boundary layer during the cavitation simulation.

Vapor volume fraction visualization with pressure drop 90 is presented bar in Figure 4.

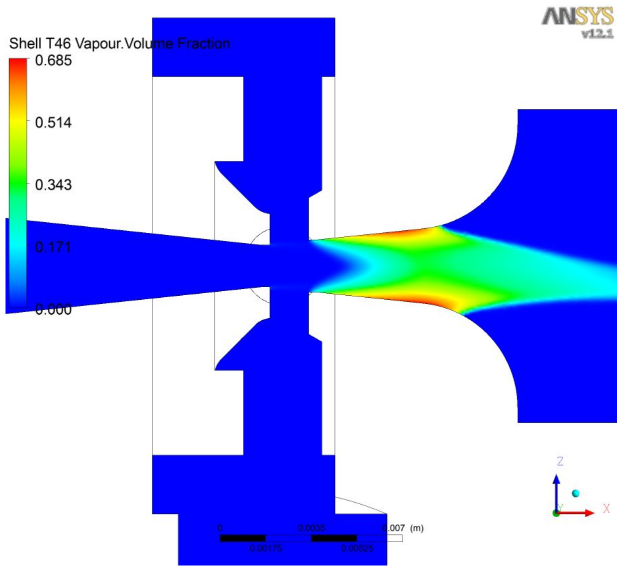

a) ZGB cavitation model

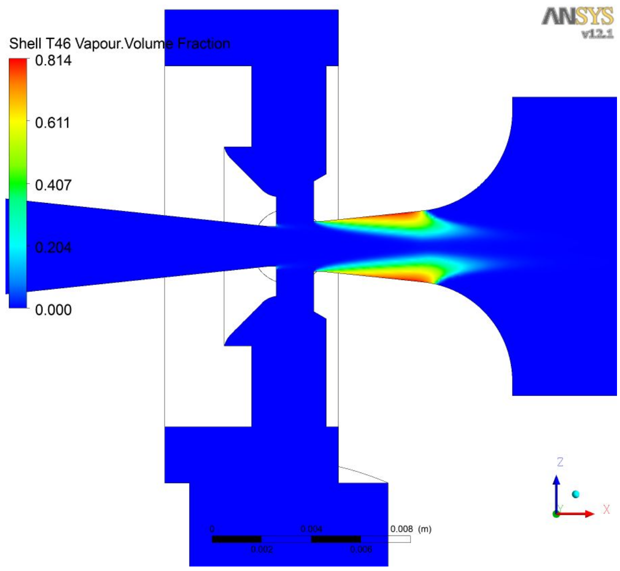

b) a new cavitation model

Figure 4. Vapor volume fraction obtained during numerical simulation of working fluid flow through jet element "pipe-pipe" with inlet pressure drop 90 bar

Figure 4 analysis shows the increase of vaporization intensity during the simulation by new cavitation model (vapor volume fraction increases from 0,68 to 0,814). Increased vaporization results in pressure field changes in a solver, which in turn results in modification of the form of the cavitation zone. The obtained form of cavitation zone is quite similar to the form observed by Acekeret (Acekeret, 1930). Comparing Figure 3 with Figure 4 we could note that the points of the flow detachment coincide with points of cavitation ending on the walls, which enables to make a conclusion about cavitation character of preservation of the boundary layer during cavitation stabilization of fluid mass flow.

During simulation with ZGB cavitation model switched on a divergence of simulation and experimental results is 5,2%, while with new cavitation model (17) divergence is 2,5%. Error of flowmeter is 1,5 – 2% from measured value.

4. Discussion

The dynamic component of the new numerical model of cavitation mass transfer fundamentally differs from the dynamic component of cavitation mass transfer models used earlier, based on a dynamics of cavitation bubble (Singhal et al., 2001; Zwart et al., 2004; Sauer et al., 2000). The new cavitation model takes into account viscosity of cavitating fluid in Reley-Plesset equation.

Making a comparison of divergence of numerical simulation with experiment for effect of cavitation stabilization of mass flow with pressure 100 bar shows that the new model has a half divergence in stabilization zone than Zwart-Gerber-Belamri model. That could be explained by taking into account the fluid viscosity (80 sSt for hydraulic oil Shell T46). Primarily Zwart-Gerber-Belamri model was verified for water and with viscosity of 1 sSt during vapor cavitation (Zwart et al. 2004).

Comparing visualization of vapor volume fraction for two separate cavitation models enables to conclude that the new cavitation model has more intensive vaporization at pressures higher than 2 MPa and less intensive vaporization at pressures lower than 2 MPa, giving a more adequate representation of cavitation zone (Acekeret, 1930). A comparison of visualization of vapor volume fraction obtained during simulation with visualization of vapor volume fraction in a Venturi tube (Sauer, 2000) shows that taking into account the viscosity enables to determine more adequately the pressure field and, respectively, flow character and cavitation zone location.

Velocity field comparison with and without taking into account the cavitation enables to propose a jet character of the effect of cavitation stabilization of mass flow. During flow simulation with cavitation model switched off (ideal flow) a jet boundary layer enters a receiving nozzle for 1 – 1,5 mm and breaks down. During flow simulation with cavitation model switched on (real flow) a jet boundary layer is retained until it separates in receiving nozzle. Thus we can suppose that the cause of the effect of cavitation stabilization of mass flow is the preservation of the jet boundary layer (in receiving nozzle – wall boundary layer) during hydrodynamic cavitation.

It should be noted that the cavitation mass transfer models based on phase transfer equations take into account the fluid viscosity (Vortmann, 2001). However, these models have a solution only for water and not applicable for hydraulic oils used in hydraulic systems.

5. Conclusion

1. Analysis of structure of numerical models of cavitation mass transfer revealed the statistical and dynamic components. Step-by-step evolution of the static component with an invariance and weakness of the dynamic component (without taking into account the viscosity and surface tension) has been discovered. Thus the dynamic component modification seems to be the most promising development of numerical models of cavitation mass transfer.

2. On basis of Reley-Plesset equation, which takes into account fluid viscosity, a method of modification of the dynamic component of numerical model of cavitation mass transfer has been developed. This method made possible to synthesize a new dynamic component. A new numerical model of cavitation mass transfer (17) has been obtained by taking into account the new dynamic component (16).

3. Verification of results of cavitation simulation with experiment shows that during simulation of effect of cavitation stabilization of mass flow the error was 5,2%, while during the simulation with the new model the error was no more than 2,5%, and that is within errors accepted. At the same time the new model is visualizing the flow more accurate and takes into account an additional parameter such as fluid viscosity.

4. Comparison of velocity fields during simulation with and without cavitation shows that the hypothesis of preservation of the jet boundary layer during the effect of cavitation stabilization of fluid mass flow is sufficient.

Acknowledgement

We are responsible for all errors as well as heavy style of the manuscript.

References

Acekeret, J. (1930). Experimentelle und teoretische Untersuchungen uber Hohlraumbuldung (Kavitation) im Wasser. *Technische mechanik und thermodynami.* Berlin, 1. ss. 1, 22. http://dx.doi.org/10.1007/bf02640226

Bocharov, V. P. (1987). *Calculation and engineering of devices of hydraulic fluidics*. Kiev: Technika.

Brennen, C. E. (1995). *Cavitation and bubble dynamics. Oxford university press.* http://dx.doi.org/10.1017/cbo9781107338760

Delale, C. F., Schnerr, G. H., & Sauer, J. (1998). Quasi-one-dimensional caviting nozzle flows. *Submittes to J. Fluid Mechanics.* http://dx.doi.org/10/1017/s0022112000002330

Gimranov, E. G., & Tselischev, V. A. (2008). *Unsteady hydro-gas-dynamic effects in systems of hydraulic and* *pneumatic actuators.* Ufa: UGATU. ISBN 978-5-86911-825-7

Knapp, R. T., Daily, J. W., & Hammitt, F. G. (1970). *Cavitation.* McGraw, Hill Book Co., 688 s.

Konstantinov, S. U., & Tselischev, D. V. (2013). Research and development of numerical models of cavitation mass transfer. *Vestnik UGATU*, *3*, 123-129. Retrieved from http://elibrary.ru/item.asp?id=20371685

Levkovsky, U. L. (1978). *Structure of cavitation flows.* Leningrad: Sudostroenie.

Markina, N. L., & Reviznikov, D. L. (2011). Numerical modeling of fluid flow in the presence of cavitation. *Vestnik MAI*, *2*, 200-210.

Nigmatullin, R. I. (1987). *Dynamics of multiphase mediums.* Moscow: Science.

Permyakov, G. S., & Tselischev, D. V. (2010). Research of effect of mass flow stabilization. *Vestnik UGATU, 2*(37), 21-29. Retrieved from http://elibrary.ru/item.asp?id=18862077

Rozhdestvesky, V. V. (1977). *Cavitation.* Leningrad: Sudostroenie.

Sauer J. (2000). Instationar kavitierende Stromungen – Ein neues Modell, basierend auf Front Capturing (VoF) und Blasendynamik. Karlsruhe, 162 s. Retrieved from http://nbn-resolving.org/urn:nbn:de:swb:90-AAA31220009

Schnerr, G. N., Vortmann, C., & Sauer, J. (1999). Numerical studies of flow in fuel injector nozzles – interaction of separation and cavitation. *Buchbeitrag zum DFG-Schwerpunktprogramm "Transiente Vorgange im mehrphasen Sustemen mit einer oder mehreren Komponenten"*, Wiley-VCH Weinheim. http://dx.doi.org/10.1002/9783527610785.ch21

Schnerr, G. H., & Sauer, J. (2001). Physical and Numerical Modeling of Unsteady Cavitation Dynamics. *In Fourth International Conference on Multiphase Flow*, New Orleans, USA. http://dx.doi.org/10.1142/9789812796837_0032

Singhal, A. K., Li, H. Y., Athavale, M. M., & Jiang, Y. (2001). Mathematical basis and validation of the full cavitation model. *Asme Fedsm'01*, New Orleans, Louisiana. http://dx.doi.org/10.1115/1.1486223

Tselischev, V. A., & Tselischev, D. V. (2006). Hydraulic machine with jet-cavitation method of control. *Vestnik UGATU*, *2*, 161-165. Retrieved from http://elibrary.ru/item.asp?id=9289636

Vortmann C. (2001). Untersuchen zur Thermodynamik des Phasenubergangs bei der numerischen Berechnung kavitierender Dusenstromungen. Karlsruhe, 132s. Retrieved from http://nbn-resolving.org/urn:nbn:de:swb:90-AAA32020011

Wallis, G. B. (1969). *One-dimensional two-phase flow.* New York: McGraw. Hill Book Co. http://dx.doi.org/10.1002/aic.690160603

Wursthorn, S. (2001). *Numerische Untersuchung kavitierender Stromungen in einer Modellkreiselpumpe*, Karlsruhe, 185s. Retrieved from http://nbn-resolving.org/urn:nbn:de:swb:90-AAA40820015

Zwart, P. J., Gerber, A. G., & Belamri, T. (2004). A Two-Phase Flow Model for Predicting Cavitation Dynamics. *In Fifth International Conference on Multiphase Flow*, Yokohama, Japan. http://dx.doi.org/10.1115/1.1454109